Applied Catalysis B: Environmental 249 (2019) 9–18

Contents lists available at ScienceDirect

Applied Catalysis B: Environmental

journal homepage: www.elsevier.com/locate/apcatb

Comparative studies of P/CeO_2 and Ru/CeO_2 catalysts for catalytic combustion of dichloromethane: From effects of H_2O to distribution of chlorinated by-products

Qiguang Dai[a,1], Jinyan Wu[a,1], Wei Deng[b], Jiasu Hu[c], Qingqing Wu[a], Limin Guo[b], Wei Sun[a], Wangcheng Zhan[a,*], Xingyi Wang[a,*]

[a] Key Laboratory for Advanced Materials, Research Institute of Industrial Catalysis, School of Chemistry and Molecular Engineering, East China University of Science and Technology, Shanghai 200237, PR China
[b] School of Environmental Science and Technology, Huazhong University of Science and Technology, Wuhan 430074, PR China
[c] Hangzhou EXPEC Technology Development Co., Ltd., Zhejiang 310052, PR China

ARTICLE INFO

Keywords:
Catalytic oxidation
CVOCs
Phosphate
Ruthenium oxide
Ceria

ABSTRACT

Phosphate- and ruthenium oxide-supported CeO_2 (P/CeO_2 and Ru/CeO_2), as typical CeO_2-based catalysts, were comparatively studied to fully elucidate catalytic combustion of dichloromethane (DCM), especially for the effects of H_2O and the formation of chlorinated by-products. The results indicated that the reversible inhibitive effect of H_2O became increasingly intense in the following order: pristine CeO_2 < Ru/CeO_2 < P/CeO_2, moreover, the inhibition was more notable at the lower reaction temperature but almost disappeared at temperatures above 300 °C. H_2O-TPD and various DRIFTS techniques revealed that the adsorption strength of H_2O depended on the surface properties of three CeO_2-based catalysts and the reaction temperature, which eventually determined the degree of activity inhibition. Dechlorinated (monochloromethane, MCM) and ploychlorinated ($CHCl_3$ and CCl_4) by-products were more easily formed over non-metallic P/CeO_2 and metallic Ru/CeO_2, respectively, due to the different redox and metallic properties of these CeO_2-based catalysts, which was also further confirmed by catalytic oxidation of other chlorinated volatile organic compounds (Cl-VOCs). Additionally, more complete oxidation (the formation of CO_2 and Cl_2) occurred on Ru/CeO_2.

1. Introduction

Chlorinated volatile organic compounds (Cl-VOCs or CVOCs) or chlorinated hydrocarbons (CHCs), such as dichloromethane (DCM), vinyl chloride (VC), epichlorohydrin (ECH), chloropropanol (CP), 1,2-dichloroethane (DCE), trichloroethylene (TCE) and chlorobenzene (CB), are extremely hazardous to the environment and human health [1–4]. Therefore, the use and emission of Cl-VOCs are widely regulated all over the world, mainly involving the manufacture of polyvinylchloride and epoxy resin, the cleaning industry (degreasing agents) and the municipal solid waste incineration (MSWI). Catalytic combustion has been considered to be a promising candidate technology for its energetic efficiency, strong handling ability and lack of secondary pollution. However, the screening of efficient catalysts (low cost, high activity, durability and selectivity) still remains challenging [5–7].

Recently, ceria (CeO_2) has been found to be highly active for catalytic combustion of Cl-VOCs but shows inevitable rapid deactivation due to easy re-dissociation and the strong adsorption of inorganic chlorine species (ICs) on active sites [8]. This problem can be solved by two pathways, as listed in Scheme 1. (1) The first is doping with transition metals (TMs, such as Mn, Cu, Fe or Co) [9,10] or loading of Ru [11,12] to remove the adsorbed ICs from active sites in the form of Cl_2. The transition metal oxides were easily chlorinated into $TMOCl_x$ or $TMCl_x$ by the substitution of oxygen with chlorine and were then re-oxidized *via* the release of oxygen from CeO_2, whereas Ru, a highly active catalyst for the Deacon reaction (oxidation of HCl into Cl_2), possessed an excellent catalytic performance for oxidation of the dissociated chlorine species into Cl_2. (2) The second pathway is the incorporation of Brønsted acidic sites (surface modified CeO_2 with V, Mo, W, PO_4^{3-}, SO_4^{2-}, or HZSM-5, *etc.*) to promote the formation of desired HCl and to inhibit the re-dissociation and adsorption of ICs on CeO_2

* Corresponding authors.
E-mail addresses: zhanwc@ecust.edu.cn (W. Zhan), wangxy@ecust.edu.cn (X. Wang).
[1] These authors contributed equally to this work.

https://doi.org/10.1016/j.apcatb.2019.02.065
Received 11 December 2018; Received in revised form 17 February 2019; Accepted 22 February 2019
Available online 23 February 2019
0926-3373/

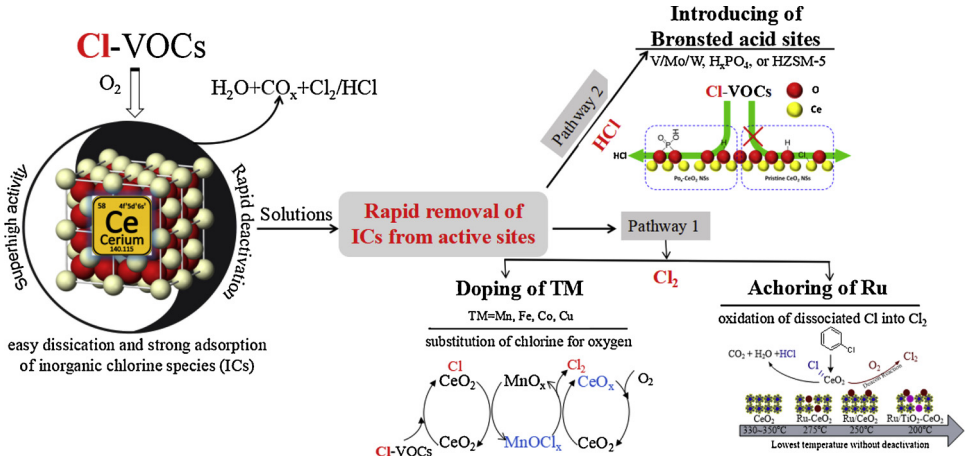

Scheme 1. Two feasible pathways proposed to solve the rapid deactivation of CeO_2 catalysts for the catalytic combustion of Cl-VOCs.

active sites [13–15]. Although the efficiency of these two pathways in improving the chlorine-resistant ability of CeO_2 was widely studied, the differences between the two pathways have rarely been explored directly, especially in regards to the formation of by-products. For example, for Pathway 1, polychlorinated by-products were still unavoidable due to the high reactivity of formed Cl_2, especially at higher temperatures. As such, the desired catalysts should be able to oxidize the dissociated chlorine species into Cl_2 at temperatures as low as possible to inhibit the deep chlorination of transition metal oxides and the subsequent polychlorination reaction. In contrast, for Pathway 2, the formation of the incompletely oxidized products, such as CO or coking, was tricky due to the lack of redox ability after introducing acid sites. Among all catalysts employed in the two pathways, CeO_2 supported nonmetallic phosphate (P/CeO_2) and noble-metallic ruthenium oxide (Ru/CeO_2) were regarded as the most representative and promising CeO_2-based catalysts, and a comparative study of their differences with regard to the oxidation of Cl-VOCs will provide valuable information for designing more efficient catalysts.

Another issue that should be comprehensively studied is the effects and/or roles of H_2O on the catalytic combustion of Cl-VOCs because H_2O not only occurs in practical flue gases but is also one of the products of Cl-VOCs combustion reactions. Generally, H_2O has exhibited inhibiting and/or deactivating effects due to its competitive adsorption with reactants on active sites, especially at low temperatures. However, a promoting effect could also be observed on certain catalysts *via* an additional hydrolysis pathway of Cl-VOCs, especially at high concentrations of H_2O [8]. On the other hand, the presence of H_2O promoted the formation of the more desired HCl product (H_2O as a hydrogen donor) and improved the chlorine tolerance of catalysts (H_2O as absorbent or stripping agents of ICs adsorbed on active sites). However, these results were not consistent or definite, and the mechanism of H_2O inhibition also had not been reported. Therefore, in this work, the differences in the effects or roles of H_2O in the catalytic combustion of Cl-VOCs using DCM as a model pollutant over CeO_2-based catalysts (P/CeO_2 and Ru/CeO_2) was intensively compared.

2. Experimental section

2.1. Catalyst preparation

Phosphate- and ruthenium oxide-modified CeO_2 nanosheets were prepared through an incipient wetness impregnation route using trimethylphosphate (TMP) and ruthenium chloride ($RuCl_3$) as precursors [12,15]. The molar ratio of P/Ce was controlled to be 0.2 and the mass content of Ru was 1%. After the impregnation, the wet samples were statically aged for 24 h at room temperature, and then dried at 80 °C and calcined at 450 °C for 4 h with a 5 °C/min ramp rate in flowing air. The as-prepared catalysts were respectively marked as P/CeO_2 and Ru/CeO_2, but the labels did not imply that P and Ru existed in the form of elemental P and metallic Ru, practically H_xPO_4 and RuO_x. The actual element atomic ratio of P/Ce was quantified to be 0.16 based on the energy dispersive spectroscopy (SEM-EDS) analysis, and the content of Ru was 0.95% as measured by X-ray fluorescence (XRF) technology.

2.2. Catalyst characterization

A temperature-programmed surface reaction (TPSR) was performed to monitor the distribution of DCM oxidation products in the absence or presence of H_2O. The sample (100 mg) was exposed to a gas stream (50 ml/min) containing 4000 mg/m^3 DCM, 20 vol. % O_2 and balanced Ar in the absence or presence of 3 vol.% H_2O and heated from 50 to 400 °C at a rate of 10 °C/min. The temperature was maintained at 400 °C for 30 min and was then naturally cooled to 125 °C. The outlet products such as CO_x, monochloromethane (MCM), $CHCl_3$, CCl_4, HCl and Cl_2, were continuously measured using a quadrupole mass spectrometer with heated quartz inert capillary (QIC) sampling system (Hiden HPR20 MS).

H_2O-temperature programmed desorption (H_2O-TPD) was performed in a quartz tube reactor system equipped with a Hiden HPR20 MS. Prior to the TPD analysis, 100 mg of the sample was first pre-heated at 400 °C in 20 vol. % O_2/Ar flow (30 ml/min) for 1 h, cooled to 50 or 100 °C, and swept by Ar for another 1 h. 3 vol.% H_2O or D_2O/Ar (30 ml/min) was introduced into the catalyst bed for 30 min. An Ar flow (30 ml/min) was then purged through the catalysts for 1 h to remove physiosorbed H_2O or D_2O. After that, the sample was heated to 500 °C at a ramp of 10 °C/min and H_2O or D_2O was continuously monitored.

The static contact angle of the as-prepared CeO_2-based film was measured by a contact angle measuring instrument (Dataphysics OCA20) to evaluate the hydrophilic-hydrophobic property of three CeO_2-based catalysts. The films of samples were fabricated by drop-casting an ethanolic suspension of samples onto a glass wafer [16].

In situ diffuse reflectance infrared Fourier transform spectra (DRIFTS) were recorded at a spectral resolution of 4 cm^{-1} on a Nicolet 6700 spectrometer equipped with an *in situ* diffuse reflectance cell containing an Mercury-Cadmium-Telluride (MCT) detector and ZnSe window. Prior to each spectrum recording, the sample was purged at 400 °C in 20 vol. % O_2/Ar for 1 h and was then cooled to 300, 200, 100 and 50 °C, while the corresponding background spectrum was recorded. Finally, the sample was exposed to a controlled steam flow (50 ml/min) containing 0.75 vol. % H_2O and 20 vol. % O_2/Ar, or 500 ppm DCM and 20 vol. % O_2/Ar in the absence or presence of 0.75 vol. % H_2O or D_2O. The adsorption/reaction spectra were recorded for various target temperatures or times by the subtraction of the corresponding background reference.

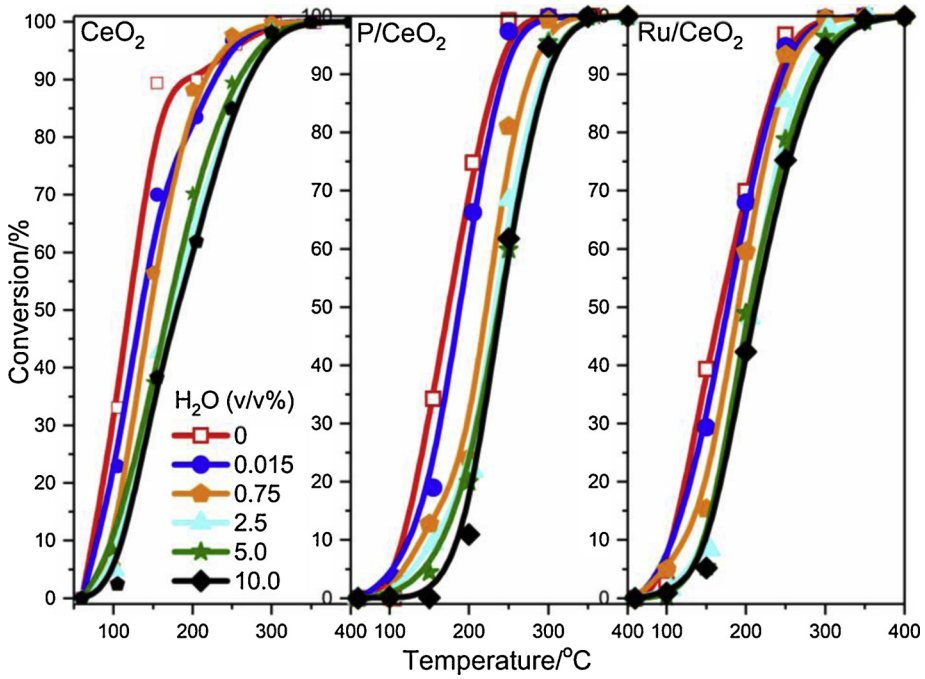

Fig. 1. Effect of H_2O contents on the catalytic combustion of DCM over pristine CeO_2, P/CeO_2 and Ru/CeO_2 catalysts. Reaction conditions: 1000 mg/m^3 DCM, 20 vol. % O_2, balanced Ar and different H_2O contents; space velocity of 15,000 ml/g h.

2.3. Activity test

Catalytic combustion of Cl-VOCs was carried out in a temperature-controlled flow micro-reactor (U-shaped quartz tube with an inner diameter of 3 mm) loading 200 mg of the as-prepared catalyst. The reactant gas composition was: 1000 mg/m^3 Cl-VOCs, 20 vol. % O_2, 0.015–10 vol. % H_2O (when used) and balanced Ar. In all the runs, the total gas flow rate was maintained at 50 ml/min (the space velocity was always fixed to 15,000 ml/g h). The effluent gases were analyzed on-line using a gas chromatography (GC) equipped with flame ionization detector (FID), and the conversion of Cl-VOCs was calculated based on the peak area after running for 15 min (sampling 3 times) at the setting temperature and the error was controlled within 0.2%.

3. Results and discussion

3.1. Effect of H_2O

Fig. 1 shows the effect of different H_2O contents on DCM conversion over three CeO_2-based catalysts. In the absence of H_2O, T_{50} and T_{90} (50% and 90% DCM conversion corresponding to the reaction temperature) were sequentially 120, 175 and 165 °C, and 200, 230 and 235 °C over pristine CeO_2, P/CeO_2 and Ru/CeO_2 catalysts, respectively. The pristine CeO_2 showed a better activity for DCM oxidation compared to P/CeO_2 and Ru/CeO_2, while the apparent activities of P/CeO_2 and Ru/CeO_2 were almost the same. The relatively poor activity of P/CeO_2 and Ru/CeO_2 might be because the loading of P or Ru occupied the partial active sites of CeO_2. It was rather remarkable that a distinct deactivation was observed over the pristine CeO_2 (an irregular S-shaped light-off curve). However, this deactivation disappeared after the introduction of P or Ru owing to the promotion of the resistance to chlorine poisoning [12,15]. When H_2O was introduced into the feeds, even at contents as low as 0.015 vol. %, the deactivation of the pristine CeO_2 was obviously alleviated, which is ascribed to the promoting effect of H_2O on removing the ICs adsorbed on active sites [17,18]. That is, the presence of H_2O could improve the stability of ceria-based catalysts for the catalytic combustion of Cl-VOCs, which was not usually found for the oxidation of other VOCs. However, a decrease in the DCM conversion could be observed with the introduction of H_2O in the feeds, and the decline in activity increased as the H_2O volume content increased. The inhibition effect of H_2O on activity was also inevitable for P/CeO_2 and Ru/CeO_2 catalysts, but with notable differences.

Fig. 2 further displays the effect of H_2O contents on DCM conversion at 100, 200 and 300 °C to more visually evaluate the differences in the three CeO_2-based catalysts. It is clear that the degree of inhibition varied with different catalysts and temperatures. The main points are summarized as follows. (1) The inhibition degree was more significant at low temperatures. The DCM conversions over pristine CeO_2, P/CeO_2 and Ru/CeO_2 catalysts decreased by 24, 64 and 27% at 200 °C, respectively, in the presence of 10 vol. % H_2O, but only decreased by 1, 5 and 3% for each catalyst at 300 °C. (2) When the H_2O content was higher than 0.75 vol. %, with a further increase in H_2O content, the decline in activity became slow. Especially for the pristine CeO_2, the decline in activity almost vanished. (3) The pristine CeO_2 and Ru/CeO_2 were more resistant to H_2O than was P/CeO_2 since the decrease in the rate of DCM conversion over P/CeO_2 became faster with water in the feeds. In brief, CeO_2-based catalysts presented a superior resistance to water especially at high temperatures, which was more valuable for their potential practical applications.

Additionally, to further study the possible deactivating behaviour of H_2O [19–21], the steady DCM conversion was compared by switching ON/OFF 0.75 vol. % H_2O at 200 and 300 °C, and shown in Fig. S1 and Fig. 3. A continuing decline in the DCM conversion with the time ageing over the pristine CeO_2 catalyst was observed in the absence or presence of H_2O, whether at 200 or 300 °C (Fig. S1), due to the rapid deactivation of pristine CeO_2 by chlorine poisoning. For P/CeO_2 and Ru/CeO_2, the introduction of H_2O caused an obvious decrease in the DCM conversion, especially for P/CeO_2 at 200 °C, which was consistent with the results from activity tests under different H_2O contents (Figs. 1 and 2). However, the DCM conversion over Ru/CeO_2 at 300 °C and over P/CeO_2 at 200 and 300 °C restored completely when H_2O was removed from the feed gas, and a slight elevation in P/CeO_2 was observed at 200 and 300 °C due to the role of H_2O in suppressing the adsorption of ICs on active sites. These results illustrated that the presence of H_2O did not poison the P/CeO_2 and Ru/CeO_2 catalysts when they reacted at certain temperature. In contrast, the activity of Ru/CeO_2 did not restore

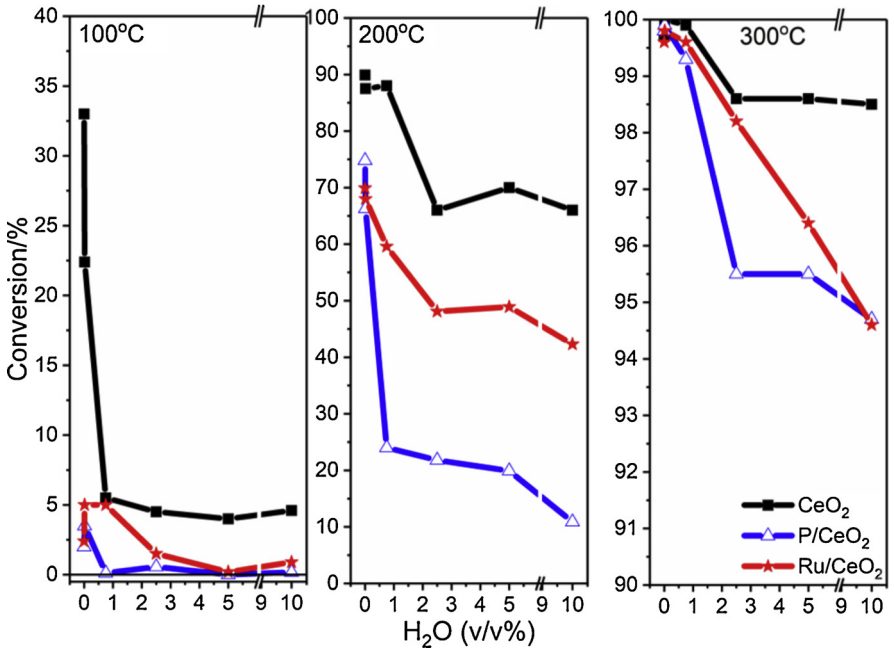

Fig. 2. Effect of H_2O contents on DCM conversion at 100, 200 and 300 °C.

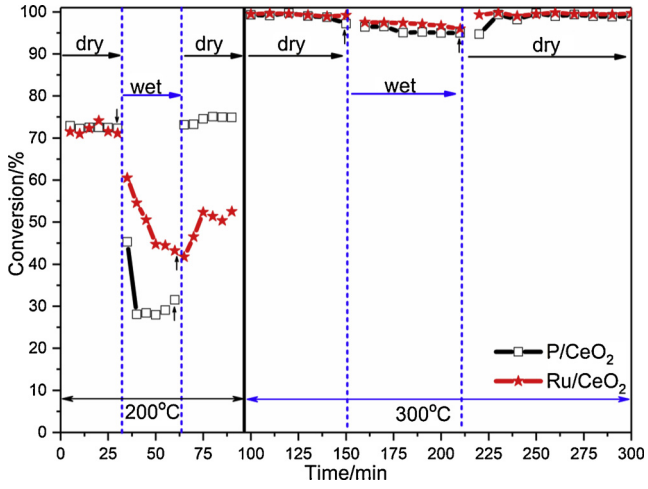

Fig. 3. Effect of H_2O on DCM conversion over P/CeO_2 and Ru/CeO_2 catalysts at 200 and 300 °C. Reaction conditions: 1000 mg/m^3 DCM, 20 vol. % O_2, 0.75 vol. % H_2O (when used), and balanced Ar; space velocity of 15,000 ml/g h.

completely at 200 °C after H_2O was OFF, a result which is attributed to deactivation caused by chlorine poisoning at low temperatures [12]. Therefore, it was concluded that P/CeO_2 presented a better low-temperature stability than Ru/CeO_2. According to a previous study [12], resistance to chlorine poisoning of catalysts in Pathway 1 (Ru/CeO_2) was achieved *via* the oxidation of ICs into Cl_2, which was more dependent on the reaction temperature and the oxidation performance of the catalysts, while the removal or desorption of HCl in Pathway 2 (P/CeO_2) to resist chlorine poisoning could occur at relatively low temperatures.

To further explore the effect of H_2O on the reaction pathway and distribution for DCM oxidation products, TPSR experiments were performed in the absence and presence of 3 vol. % H_2O. Fig. 4 displays the changes in DCM, H_2O (in the absence of H_2O) and three other groups of products including CO_x (CO_2 and CO), organic chlorinated products (MCM, $CHCl_3$ and CCl_4) and inorganic chlorine (HCl and Cl_2) *versus* temperature. First, the descending DCM profiles reconfirmed that the pristine CeO_2 was more active than the P/CeO_2 and Ru/CeO_2 catalysts, and meanwhile, deactivation was also observed. Second, two evolution peaks of CO_2 were observed over the pristine CeO_2. The low-temperature peak was mainly ascribed to desorption of CO_2 that had been adsorbed on the weak basic sites of CeO_2; the latter was the product of the complete oxidation of DCM. Meanwhile, CO was also detected during the test over pristine CeO_2, but disappeared at higher temperatures due to the complete oxidation of DCM. However, the distribution of CO_2 and CO over P/CeO_2 and Ru/CeO_2 for DCM combustion was significantly different than that over pristine CeO_2. For P/CeO_2, both CO_2 and CO were continuously monitored and CO did not vanish, even at the high temperatures (400 °C), because of the poor redox ability of P/CeO_2, which destroyed CeO_2 properties (such as adsorption and activation of oxygen) due to the introduction of phosphate. In contrast, for Ru/CeO_2, only CO_2 was observed during the reaction process, which was attributed to the high redox ability of the supported Ru catalyst [22]. Third, the products of HCl and Cl_2 for DCM oxidation were detected for all three catalysts, even though the formation time or temperature was different. The formation of HCl was observed after 37, 31 and 22 min for the pristine CeO_2, Ru/CeO_2 and P/CeO_2, respectively, and Cl_2 formed after 36, 28 and 32 min (Fig. S2). The formation of HCl or Cl_2 over pristine CeO_2 was hysteretic compared to P/CeO_2 and Ru/CeO_2 catalysts, indicating that the removal of ICs from active sites was delayed over pristine CeO_2 and then led to the deactivation of pristine CeO_2. Interestingly, the formation of HCl over P/CeO_2 was earlier than Cl_2, while the formation of Cl_2 over Ru/CeO_2 was earlier than HCl, confirming that HCl formed and was removed easily over P/CeO_2; and *vice versa,* Cl_2 over Ru/CeO_2. This result was highly consistent with the proposed pathways in Scheme 1. Fourth, different organic chlorinated by-products were monitored over various catalysts. Only MCM as a dechlorinated by-product was found over pristine CeO_2 and P/CeO_2, while polychlorinated products such as $CHCl_3$ and CCl_4 were detected over Ru/CeO_2 (the details are discussed in Section 3.2).

On this basis, the effect of H_2O in the feed gas on the distribution of DCM oxidation products was detected for all three catalysts. By adding 3 vol. % H_2O to the feed gas, the types of products, such as CO_2, CO, MCM, $CHCl_3$ and CCl_4, did not vary, indicating that the presence of H_2O did not change the reaction pathway of DCM oxidation for the three catalysts. However, the concentration of some products changed under the feed gas that contained H_2O. For example, the formation of MCM over P/CeO_2 was suppressed, while the formation of $CHCl_3$ and CCl_4

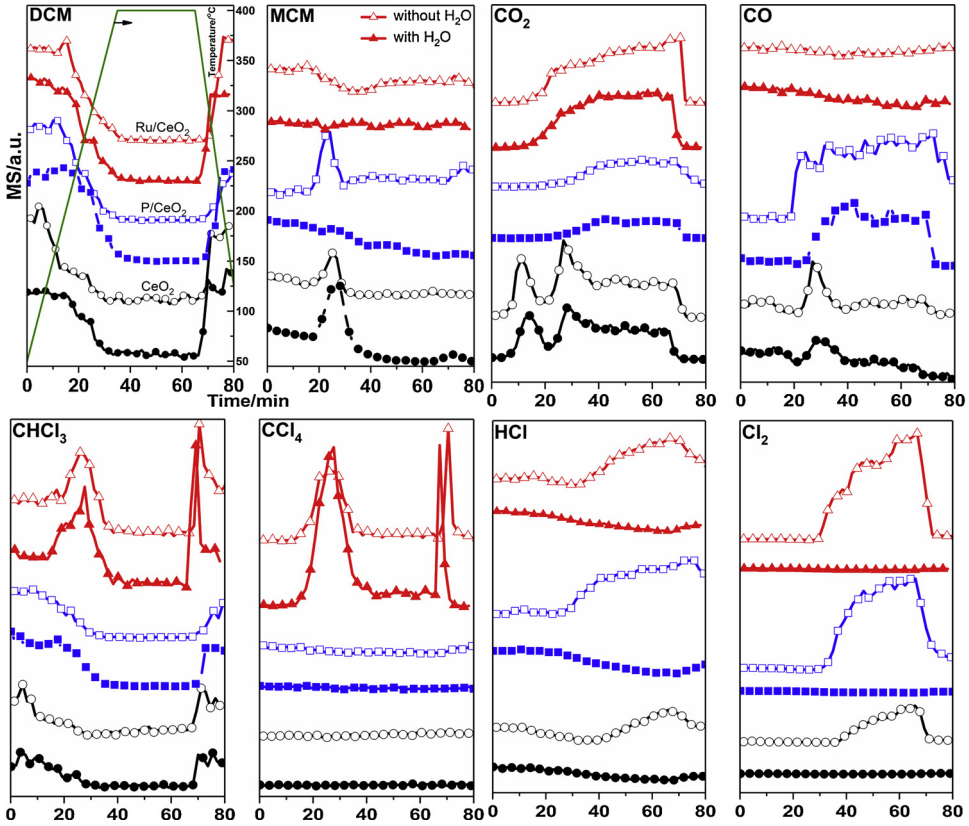

Fig. 4. TPSR of DCM oxidation over pristine CeO_2, P/CeO_2 and Ru/CeO_2 in the presence and absence of H_2O. Reaction conditions: 4000 mg/m^3 DCM, 20 vol. % O_2, 3 vol. % H_2O (when used), and balanced Ar; space velocity of 30,000 ml/g h. Dotted lines: in the absence of H_2O, solid lines: in the presence of H_2O.

over Ru/CeO_2 was promoted; in addition, the amount of CO over pristine CeO_2 and P/CeO_2 decreased slightly due to the water gas-shift reaction (CO + H_2O→CO_2 + H_2) [23]. Puzzlingly, either HCl or Cl_2 was not detected in the presence of H_2O over all three catalysts, which could be attributed to their highly solubility in H_2O due to the condensation of water vapor in filter tap located before QIC sampling system.

In summary, the presence of H_2O obviously decreased the catalytic activity of three CeO_2-based catalysts for DCM oxidation, and the inhibition degree was in the following sequence: CeO_2 < Ru/CeO_2 < P/CeO_2. However, this passive effect can be relieved when the water content was increased to higher than 0.75 vol. % and the reaction temperature was higher than 300 °C. Additionally, the inhibition effect of H_2O was reversible (not the poisoning deactivation), and the reaction pathway was not changed by the addition of H_2O in the feed gas. The behaviour and the influence mechanism of H_2O during the reaction is further discussed in the following sections.

Generally, the decrease in DCM conversion that resulted from the presence of H_2O was attributed to the competitive adsorption of H_2O with DCM and/or O_2. Thus, the adsorption/desorption of H_2O on catalysts' surfaces was first investigated by H_2O-TPD, contact angle (hydrophilic-hydrophobic property) and DRIFT spectra (H_2O adsorption and H_2O-DCM co-adsorption). The desorption behaviours of H_2O (pre-adsorbed at 50 and 100 °C) *versus* temperature over catalysts are illustrated in Fig. 5. Desorption peaks were observed at 115, 135 and 145 °C (pre-adsorbed at 50 °C) over CeO_2, P/CeO_2 and Ru/CeO_2, respectively (verified by D_2O-TPD, Fig. 5 inset), while the corresponding desorption peaks shifted to 155, 195 and 185 °C over catalysts when H_2O was pre-adsorbed at 100 °C. Moreover, compared to pristine CeO_2, the initial desorption temperature over P/CeO_2 and Ru/CeO_2 was increased by 10 °C, and the peak was obviously broadened. The full widths at half maximum (FWHM) of pristine CeO_2, P/CeO_2 and Ru/CeO_2 were 46, 110 and 80, respectively. These results indicated that the

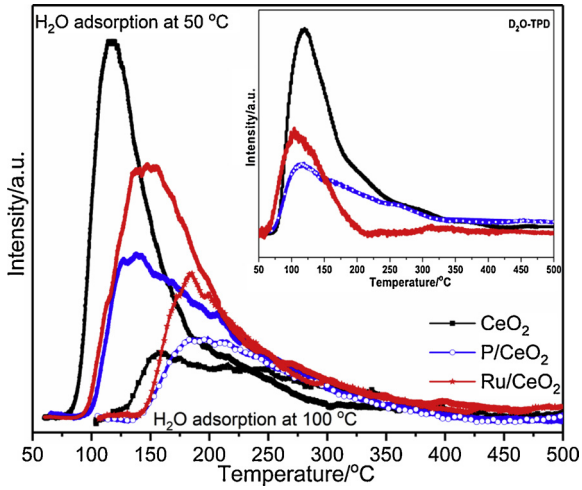

Fig. 5. TPD of H_2O and D_2O adsorbed on pristine CeO_2, P/CeO_2 and Ru/CeO_2 catalysts.

supported P or Ru increased the strength of H_2O adsorption. In other words, H_2O was more easily and strongly adsorbed on P/CeO_2 and Ru/CeO_2 compared to the pristine CeO_2. In contrast, the complete desorption of H_2O over three catalysts was almost achieved above 300 °C, which was responsible for the negligible inhibition effect of H_2O on the catalytic oxidation of DCM at 300 °C. On the other hand, the amount of H_2O from the CeO_2 and Ru/CeO_2 catalysts was almost the same, but higher than that of P/CeO_2. However, when H_2O was pre-adsorbed at a higher temperature of 100 °C, the desorption amount of H_2O over pristine CeO_2 decreased significantly due to the weaker adsorption of H_2O on pristine CeO_2. Moreover, the static contact angle measurement

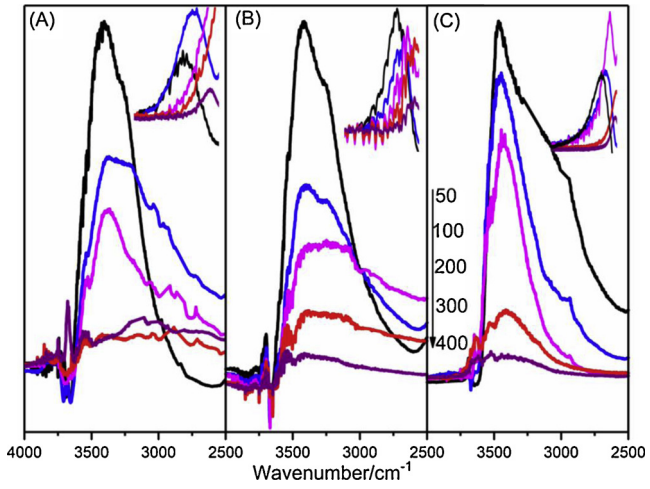

Fig. 6. *In situ* DRIFT spectra of H_2O adsorption (0.75 vol. % H_2O) over (A) CeO_2, (B) P/CeO_2 and (C) Ru/CeO_2 catalysts at different temperatures (inset, bands at 1630–1650 cm^{-1}).

showed that the contact angles of pristine CeO_2, P/CeO_2 and Ru/CeO_2 were 12.4, 16.3 and 15.8°, respectively, indicating that the prepared catalysts were extremely hydrophilic (Fig. S3). In conclusion, the inhibition of H_2O on activity of catalysts for DCM combustion (P/CeO_2 > Ru/CeO_2 > pristine CeO_2) was more depended on the adsorption strength of H_2O compared to the adsorption amount of H_2O.

The infrared spectroscopy technique has become a simple and sensitive method used to explore surface adsorption species under *in situ* conditions, and herein was used to study the possible competitive adsorption of H_2O with DCM. Generally, the stretching vibration (bending vibration) of O—H existing in free, adsorbed, crystal and structural water presented characteristic bands at 3756 (1595), 3435 (1630), 3200–3250 (1670–1685) and 3640 (1350–1260) cm^{-1}, respectively [24]. Specifically, the band centred at 3430 cm^{-1} (in the range of 2800 and 3600 cm^{-1}) can be used to study the adsorption of H_2O on the possible active sites for DCM oxidation, such as $Ce^{3+/4+}$ sites and oxygen vacancies. Fig. 6 presents *in situ* DRIFT spectra of H_2O adsorption at different temperatures in the presence of 0.75 vol. % H_2O. For all catalysts, the intensity of this band decreased as temperature increased, especially at temperatures higher than 200 °C, indicating that the adsorption of H_2O on the catalyst surface was weakened and/or the desorption rate of adsorbed H_2O became fast at elevated temperatures. This result was in consistent with the results of H_2O-TPD. Therefore, it is concluded that the competitive adsorption of H_2O with DCM might not occur or very weak at high temperatures, and thus the inhibition effect of H_2O on the catalytic activities of catalysts was alleviated. Additionally, negative bands at 3600–3700 cm^{-1} were usually detected if an adsorbate on the surface of CeO_2-based catalysts and OH groups on the catalyst surface were consumed [15,24,25]. Since these reversal peaks were absent over three catalysts, it was revealed that the adsorption of H_2O on surface OH sites did not occur.

Fig. S4 further displays *in situ* DRIFT spectra of DCM and H_2O co-adsorption over catalysts with pre-adsorbed H_2O at 50 °C. To quantitatively evaluate the adsorption/desorption of H_2O, the ratio of the peak area of the absorbed H_2O at different temperatures and that at 50 °C ($A_{T,\ H2O}/A_{50,\ H2O}$) was calculated based on Fig. 6 and Fig. S4, as shown in Fig. 7. The absorption/desorption behaviours of H_2O *versus* temperature in the co-presence of DCM and H_2O was similar to those in the absence of DCM. The intensity of bands reduced as temperature increased, especially above 300 °C. More specifically, after the gas mixture of DCM and H_2O was introduced into the catalysts with pre-adsorbed H_2O at 50 °C, the amount of adsorbed H_2O over pristine CeO_2 and Ru/CeO_2 declined more rapidly than that in the absence of DCM as temperature increased. This result indicated that DCM presented a strong competitive effect on H_2O adsorption over pristine CeO_2 and Ru/CeO_2, and DCM was more easily or strongly adsorbed on the surfaces of the two catalysts. However, the decline in the amount of adsorbed H_2O over the P/CeO_2 catalyst occurred more slowly in the presence of DCM, illustrating that the introduction of DCM had a weak influence on the adsorption of H_2O over P/CeO_2 catalyst. It was noteworthy that the introduction of phosphate on the CeO_2 surface can facilitate abundant surface P—OH groups and that the adsorption of DCM on the surface OH groups led to the appearance of the new broad band in the 3200–3600 cm^{-1} region due to the formation of hydrogen bonds (adsorbed DCM interacts with the surface OH groups *via* —O—H···$ClCH_2Cl$) [25]. Meanwhile, the negative bands at 3600–3700 cm^{-1} were detected over all catalysts and are attributed to the adsorption of DCM on surface OH groups. Thus, it was deduced that the adsorption of DCM on catalysts occurred easily, even in the co-presence of H_2O. In general, the competitive adsorption between H_2O and DCM on surface OH groups did not exist (as shown in Fig. 6), and the OH groups were not active sites for DCM oxidation. Additionally, *in situ* DRIFT spectra of DCM oxidation *versus* temperature (Fig. S5–7) accompanied by DCM and H_2O co-adsorption/oxidation over catalysts with pre-adsorbed DCM (Fig. S8) was conducted. The results confirmed that the adsorption of H_2O on P/CeO_2 was stronger than that on CeO_2 and Ru/CeO_2, leading to a more competitive adsorption on DCM and stronger inhibition effect to the reaction for P/CeO_2.

When H_2O and DCM were co-adsorbed on catalysts with pre-adsorbed H_2O or DCM (Fig. S4 and S8), the bands corresponding to adsorbed H_2O (centred at 3430 cm^{-1}, in the range of 2800 and 3600 cm^{-1}) were broad and weak. Meanwhile, a broad band in the range of 3200–3600 cm^{-1} also appeared due to the adsorption of DCM on surface OH groups (—O—H≡$ClCH_2Cl$), which caused ambiguous results. To distinguish the difference, D_2O was employed to exchange the surface water and hydroxyl groups, and co-adsorption of DCM and D_2O was investigated. Fig. 8 shows DRIFT spectra of D_2O adsorption (0.75 vol. % D_2O) *versus* time over three catalysts at 50 °C. When put in contact with the D_2O, the bands assigned to adsorbed H_2O and surface hydroxyl groups disappeared quickly (the negative bands at 3600–3700 cm^{-1} and 1630 cm^{-1} were detected), but a broad band assigned to OD stretching (2800–1800 cm^{-1}) appeared over CeO_2. For P/CeO_2, this band split into two bands at 2490 and 2320 cm^{-1}, indicating the existence of different kinds of hydroxyl groups. However, a symmetrical and sharp band cantered at 2520 cm^{-1} was detected over Ru/CeO_2 [26]. These results showed that H/D exchange could occur quickly and that the OH groups could be replaced completely by OD in 30–60 min. It should be noted that only one negative band at 3650–3670 cm^{-1} (the bridged acidic OH groups) was observed, probably because the isolated basic OH groups were difficult to exchange or were depleted during the introduction of P and Ru. After completing the H/D exchange (60 min), the DCM was introduced, and DRIFT spectra at different temperatures were recorded (Fig. 8A'–C'). The intensity of the band that corresponded to OD stretching over all catalysts decreased as temperature increased, indicating that the depleted/desorbed OD groups or adsorbed D_2O with the increase of temperature could not be replenished, even in the presence of D_2O. In other words, the adsorption of water was weak at elevated temperature. Meanwhile, it could be found that the adsorption of water over P/CeO_2 was stronger, which was consistent with the results of DCM and H_2O co-adsorption. In brief, the adsorption behaviours of H_2O and DCM over three catalysts was strongly confirmed.

3.2. Formation of chlorinated by-products

For the catalytic combustion of Cl-VOCs, the desired products were CO_2, H_2O and HCl/Cl_2. Unfortunately, chlorinated by-products were inevitable, especially polychlorinated hydrocarbons, and even dioxin. Fig. 9 shows the distribution of chlorinated products associated with DCM oxidation over CeO_2-based catalysts with or without H_2O in the

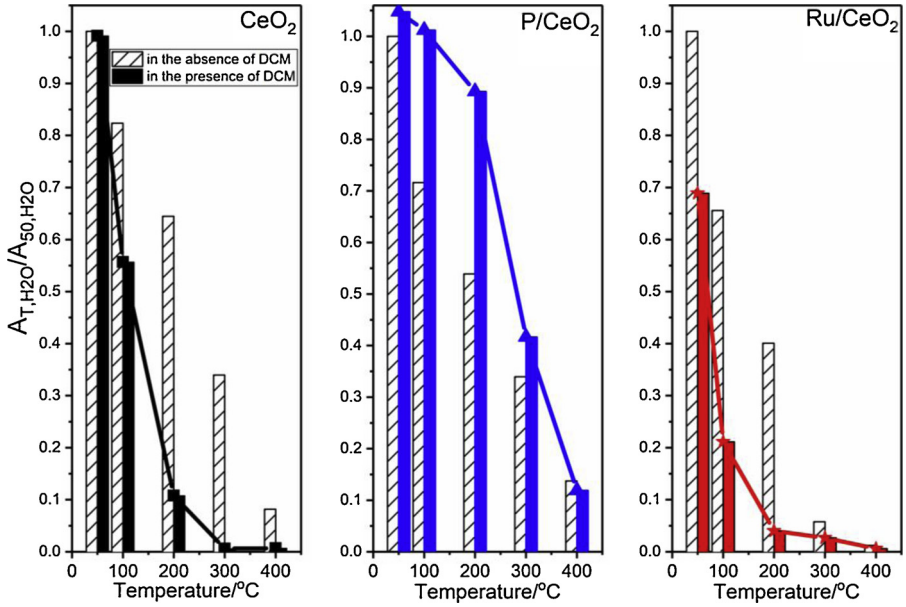

Fig. 7. The peak area ratio of the band corresponding to absorbed H_2O (centered at approximately 3430 cm^{-1}) *versus* temperature in the absence and presence of DCM.

feed gas. For pristine CeO_2, no chlorinated by-products were detected, whether in a dry or wet atmosphere. However, dechlorinated by-product such as MCM (hydrogenation and dechloridation) was observed over the P/CeO_2 catalyst, while polychlorinated by-products such as $CHCl_3$ and CCl_4 (chloridation and dehydrogenation) were observed over the Ru/CeO_2 catalyst. This phenomenon indicated that the distribution and types of chlorinated by-products depended on the properties of the CeO_2-based catalysts. The superior selectivity of pristine CeO_2 benefited from its appropriate redox ability and medium-strong basicity. After the introduction of P species on the CeO_2 surface, the decline in redox ability and enhancement in the medium-strong basicity of CeO_2 resulted in the formation of MCM as a dechlorinated by-product over the P/CeO_2 catalyst [15]. Generally, chlorinated methane, such as MCM, DCM, $CHCl_3$ and CCl_4, was formed *via* radical substitution (direct chlorination using chlorine) or oxychlorination (hydrogen chloride in combination with oxygen) of CH_4 or mono-, di- and trichlorinated methane. For these two pathways, the former (as chain propagation reaction) resulted in the formation of stepwise chlorinated methane (MCM, DCM, $CHCl_3$ and CCl_4), while $CHCl_3$ and CCl_4 were not formed for the latter pathway [27,28]. Thus, the formation of $CHCl_3$ and CCl_4 over Ru/CeO_2 was considered to be more inclined to the radical substitution pathway, because the introduction of Ru enhanced the redox ability and then resulted in the formation of more highly reactive Cl_2.

On the other hand, MCM was obviously suppressed over P/CeO_2 in the presence of H_2O, and almost disappeared as H_2O content was increased in the feed gas, which was possibly attributed to the competitive dissociation of H_2O with DCM on the medium-strong basicity sites (O^{2-}). For the Ru/CeO_2 catalyst, the presence of H_2O promoted the formation of $CHCl_3$ and CCl_4, and the trend was highly in line with the water content in the feed gas. In general, the formation of polychlorinated by-products such as DCE and TCE during the catalytic combustion of Cl-VOCs was suppressed in the presence of H_2O due to the inhibition effect of H_2O as a hydrogen source on the reactivity of Cl_2 [11,13]. It has been reported that water can improve the resistance of CeO_2-based catalysts against bulk chlorination but has almost no impact on its activity with regard to the Deacon reaction [29]. Thus, a clean catalyst surface was favourable to the generation of chlorine radicals and polychlorinated products. Additionally, the presence of H_2O inhibited the adsorption and activation of O_2 (decreasing redox ability) and the re-oxidation of the formed $CHCl_3$ and CCl_4, which resulted in enhanced selectivity of $CHCl_3$ and CCl_4.

The carbon fragments were also crucial and specially concerned in addition to the C—Cl bonds (strength and number) for the catalytic combustion of Cl-VOCs, which determined the formation of chlorinated by-products or coking. Therefore, catalytic combustion of different kinds of chlorinated hydrocarbons was investigated over CeO_2, P/CeO_2 and Ru/CeO_2 catalysts, such as chlorinated multi-carbon alkanes (1,2-dichloroethane, DCE), alkenes (vinyl chloride, VC), aromatic hydrocarbons (chlorobenzene, CB) and oxygen-containing hydrocarbons (epichlorohydrin, ECH). The activities and product distributions are shown in Fig. 10. As shown in Fig. 10A, the activity order of different Cl-VOCs (T_{90}) is as follows: ECH (145 °C) > DCM (190 °C) > DCE (230 °C) ≈ CB (230 °C) > VC (310 °C) over pristine CeO_2; ECH (145 °C) > DCE (230 °C) > DCM (235 °C) > CB (335 °C) > VC (390 °C) over P/CeO_2; and ECH (100 °C) > VC (160 °C) > DCE (200 °C) > CB (210 °C) > DCM (235 °C) over Ru/CeO_2. It was observed that the catalytic activity of CeO_2-based catalysts notably depended on the molecular structure of Cl-VOCs and the properties of catalysts (redox and acid-base properties). ECH was the most easily oxidized of all catalysts due to its structural instability (epoxide ring), while other Cl-VOCs were varied with different catalysts. In summary, pristine CeO_2 and P/CeO_2 showed better performances for catalytic combustion of chlorinated alkanes compared to chlorinated alkenes and aromatics, especially P/CeO_2. A possible reason was that the unsaturated C—C bonds in chlorinated alkenes and aromatics were difficult to split, oxidize over pristine CeO_2 and P/CeO_2 due to the lack of strong oxidizing ability and were sequentially accompanied with the polymerizing or coking. In contrast, Ru/CeO_2 showed a super-high catalytic activity for chlorinated alkenes, but a lower activity for chlorinated alkanes. However, compared to pristine CeO_2 and P/CeO_2, Ru/CeO_2 presented a better performance for the catalytic combustion of different Cl-VOCs.

In addition to the variation in degradation efficiency of different Cl-VOCs with different CeO_2 based catalysts, the by-product distributions were also variable (Fig. 10B). For the catalytic combustion of DCE, VC and CB over the Ru/CeO_2 catalyst, no chlorinated or non-chlorinated by-products were detected, indicating the superior comprehensive performance (high activity and selectivity) of Ru/CeO_2 for the catalytic combustion of Cl-VOCs. However, VC, ethyne and benzene (B) were observed as the main products during the catalytic combustion of DCE, VC and CB over CeO_2 and P/CeO_2 catalysts. In addition, P/CeO_2

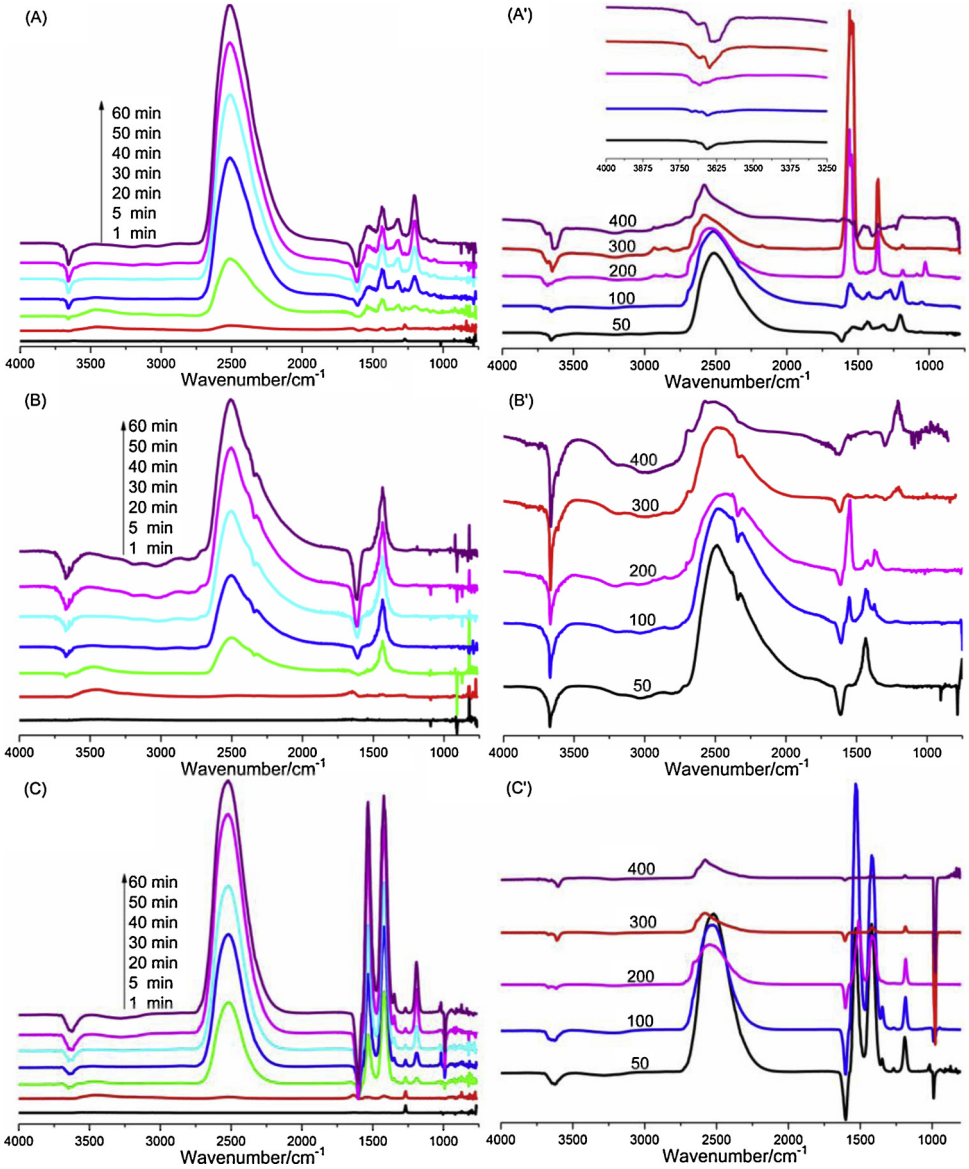

Fig. 8. *In situ* DRIFT spectra of D_2O adsorption over (A) CeO_2, (B) P/CeO_2 and (C) Ru/CeO_2 catalysts *versus* time at 50 °C (0.75 vol. % D_2O), and *In situ* DRIFT spectra of DCM oxidation over deuterated (A') CeO_2, (B') P/CeO_2 and (C') Ru/CeO_2 catalysts at different temperatures.

presented a higher selectivity of these by-products, with the exception of CB over pristine CeO_2. The former two were dehydrochlorinated by-products, whereas the latter was a dechlorinated and hydrogenated by-product (similar to the transformation of DCM to MCM). The formation of such chlorinated by-products was closely related to the redox-acid-base properties of catalysts and was more dependent on the oxidation ability. For the catalytic combustion of ECH, various and large amounts of by-products were observed over the three catalysts due to the high reactivity of ECH with an epoxy bond. The by-products were divided into two types, *i.e.*, pre- and post-products (the GC peaks appearing before and behind ECH). The amount of by-products formed increased over pristine CeO_2, Ru/CeO_2 and P/CeO_2 catalysts, in sequence. Therefore, P/CeO_2 presented a super-high selectivity for the catalytic combustion of ECH due to the presence of abundant acid sites and the decline in redox ability. More importantly, all by-products almost disappeared above 300 °C. Definitely, the ploychlorinated by-products were more easily formed over Ru/CeO_2 while dechlorinated by-products over P/CeO_2 due to the synergetic effect of redox ability, metallic or non-metallic features, and acid-base properties.

4. Conclusions

As typical and promising catalysts for the catalytic combustion of Cl-VOCs in the practical application, both Ru/CeO_2 and P/CeO_2 catalysts presented superior activity and durability (achieved *via* two different pathways). However, the differences in chlorinated by-products and tolerance to water between the non-metallic and metallic modification of pristine CeO_2 were indistinct. In this work, the catalytic combustion of DCM over Ru/CeO_2 and P/CeO_2 catalysts was comparatively investigated, with main focus on the effect or role of H_2O and the formation of chlorinated by-products. The results indicated that the inhibition of H_2O on DCM oxidation was evident and was enhanced in the following order: pristine CeO_2, Ru/CeO_2 and P/CeO_2. However, the inhibition was reversible (not poisoning deactivation), and almost disappeared at higher temperatures (300 °C), indicating that H_2O exerted a limited and solvable inhibition effect over CeO_2-based catalysts for the catalytic combustion of Cl-VOCs. H_2O-TPD and *in situ* DRIFT spectra confirmed that the adsorption strength of H_2O over the surfaces of the catalysts determined the inhibition effect of H_2O, but the competitive adsorption of DCM and H_2O on surface hydroxy groups was not

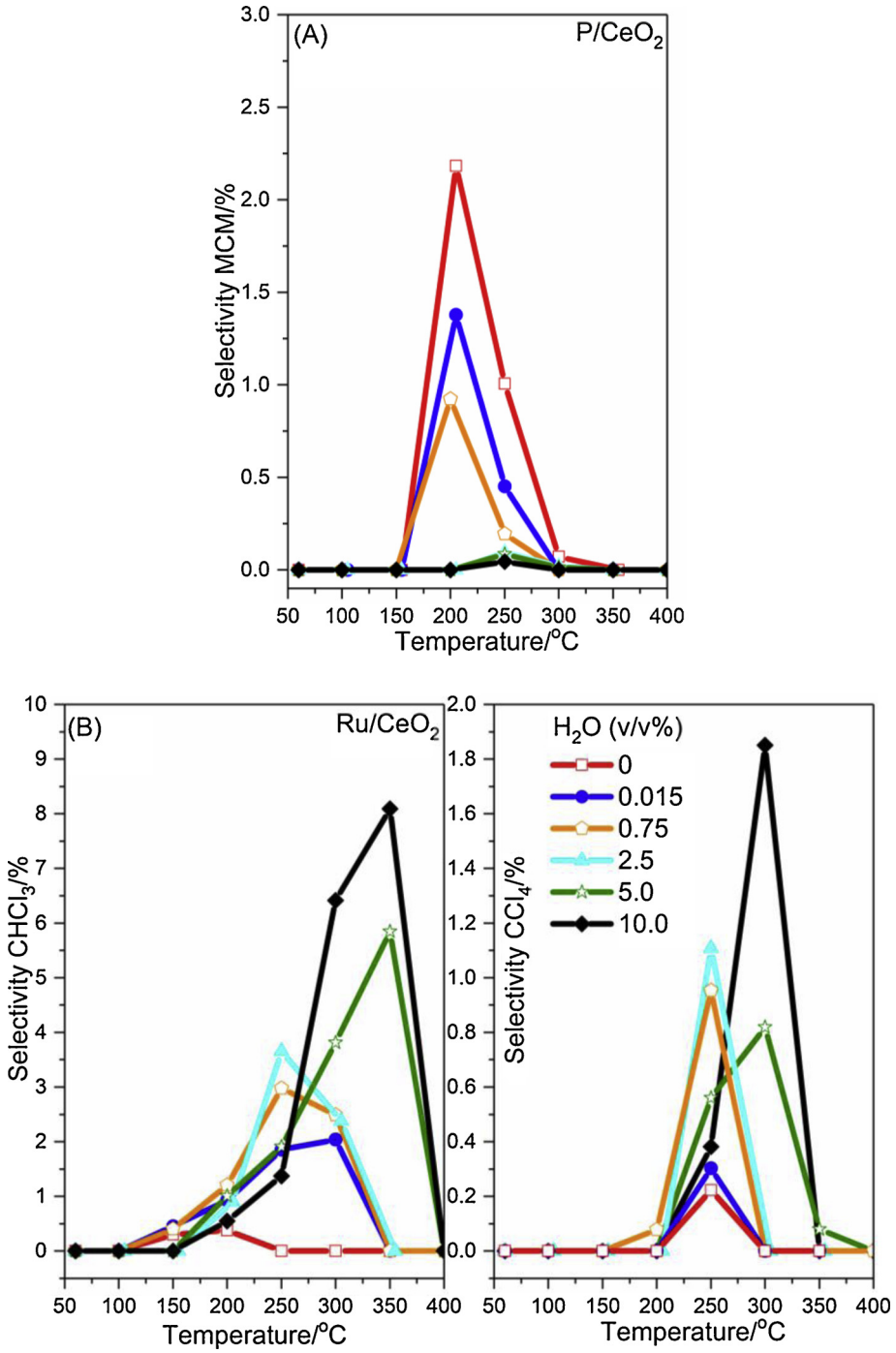

Fig. 9. Effect of H_2O on the distribution of chlorinated products of DCM catalytic combustion over P/CeO_2 (A) and Ru/CeO_2 (B) catalysts.

observed. Additionally, the presence of H_2O favoured the removal of adsorbed ICs and improved activity and durability, especially at lower H_2O contents. TPSR results indicated that the presence of H_2O in the feed gas did not change the reaction pathways but influenced the selectivity of products. As a result, MCM was obviously suppressed over P/CeO_2 and almost disappeared as H_2O increased, while the formation of $CHCl_3$ and CCl_4 was promoted over the Ru/CeO_2 catalyst. On the other hand, the P/CeO_2 and Ru/CeO_2 catalysts presented superior activities for the catalytic combustion of different chlorinated hydrocarbons, such as chlorinated alkanes, alkenes, aromatics and oxygen-containing hydrocarbons; however, obvious differences in catalytic activities and by-products were also observed. Briefly, the Ru/CeO_2 catalyst showed a better performance (higher degradation efficiency and selectivity of CO_2) compared to the P/CeO_2 catalyst. The former catalyst displayed a higher selectivity of polychlorinated by-products, while the dechlorinated by-products were more easily formed over the latter catalyst due to the synergetic effects of redox ability and acid-base properties prompted by Ru or P modification. Based on the above results, a possible basic principle can be proposed: a well-designed catalyst for the catalytic combustion of Cl-VOCs should be abundant in redox and acid sites but also deficient in base sites and resistant to bulk chlorination. Thus, it can be speculated that A/O-CeO_2 (A = P, V, Mo or W; O = Ru, Pt, Pd, Cr, Cu, Fe, Co, Ni, or Mn) catalysts due to the enhancement of acidity and oxidizing ability will be more promising for catalytic combustion of Cl-VOCs, even Cl-VOCs mixed with other non-chlorinated VOCs, but P/Ru-CeO_2 is most desirable due to the non-

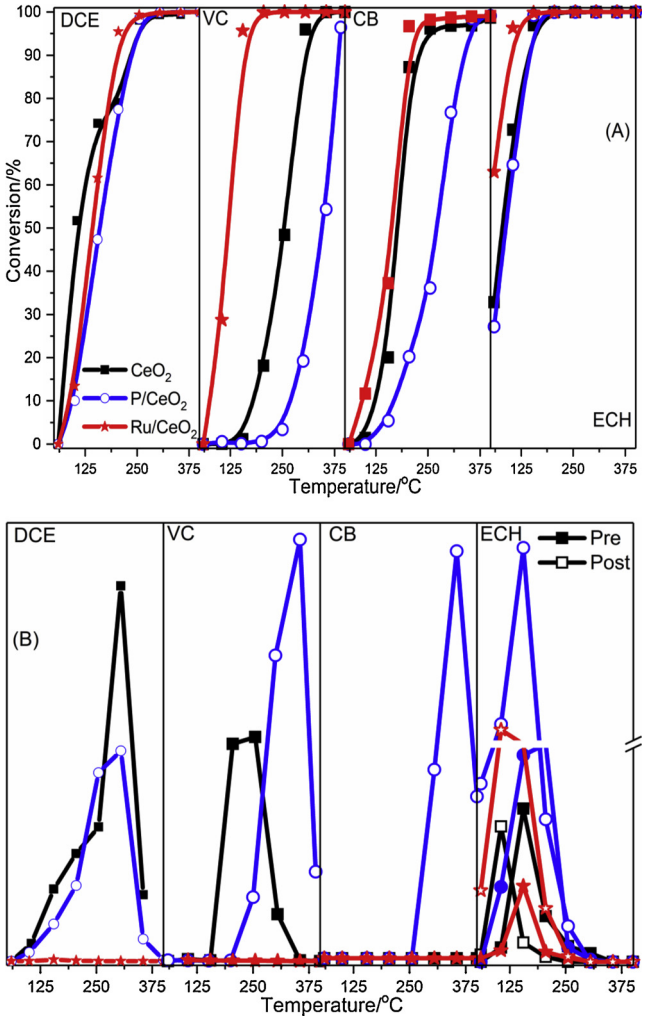

Fig. 10. Light-off cures (A) and by-product distributions (B) of different Cl-VOCs over CeO_2, P/CeO_2 and Ru/CeO_2 catalysts. Reaction conditions: 1000 mg/m^3 Cl-VOCs, 20 vol. % O_2, balanced Ar; space velocity of 15,000 ml/g h.

metallic property of phosphate and the superior chemical stability of RuO_2 (Fig. S9). These speculations should guide future efforts associated with advanced catalyst design for the catalytic combustion of Cl-VOCs.

Acknowledgements

This work was supported by the National Key Research and Development Program of China (No. 2016YFC0204300), the National Natural Science Foundation of China (No. 21777043) and Shanghai Pujiang Program.

Appendix A. Supplementary data

Supplementary material related to this article can be found, in the online version, at doi:https://doi.org/10.1016/j.apcatb.2019.02.065.

References

[1] B.B. Huang, C. Lei, C.H. Wei, G.M. Zeng, Chlorinated volatile organic compounds (Cl-VOCs) in environment-sources, potential human health impacts, and current remediation technologies, Environ. Int. 71 (2014) 118–138.
[2] L.F. Liotta, H.J. Wu, G. Pantaleo, A.M. Venezia, $Co3O_4$ nanocrystals and $Co3O_4$-MOx binary oxides for CO, CH_4 and VOC oxidation at low temperatures: a review, Catal. Sci. Technol. 3 (2013) 3085–3102.
[3] J.J. Li, R.J. Lu, B.J. Dou, C.Y. Ma, Q.H. Hu, Y. Liang, F. Wu, S.Z. Qiao, Z.P. Hao, Porous graphitized carbon for adsorptive removal of benzene and the electro-thermal regeneration, Environ. Sci. Technol. 46 (2012) 12648–12654.
[4] C. He, Z.Y. Jiang, M. Ma, X.D. Zhang, M. Douthwaite, J.W. Shi, Z.P. Hao, Understanding the promotional effect of Mn_2O_3 on micro-/mesoporous hybrid silica nanocubic-supported Pt catalysts for the low-temperature destruction of methyl ethyl ketone: an experimental and theoretical study, ACS Catal. 8 (2018) 4213–4229.
[5] A. Aranzabal, B. Pereda-Ayo, M. González-Marcos, J. González-Marcos, R. López-Fonseca, J. González-Velasco, State of the art in catalytic oxidation of chlorinated volatile organic compounds, Chem. Pap. 68 (2014) 1169–1186.
[6] M.L. Hitchman, R.A. Spackman, N.C. Ross, C. Agra, Disposal methods for chlorinated aromatic waste, Chem. Soc. Rev. 24 (1995) 423–430.
[7] W.C. Zhan, Y. Guo, X.Q. Gong, Y.L. Guo, Y.Q. Wang, G.Z. Lu, Current status and perspectives of rare earth catalytic materials and catalysis, Chin. J. Catal. 35 (2014) 1238–1250.
[8] Q.G. Dai, X.Y. Wang, G.Z. Lu, Low-temperature catalytic combustion of trichloroethylene over cerium oxide and catalyst deactivation, Appl. Catal. B-Environ. 81 (2008) 192–202.
[9] H.F. Li, G.Z. Lu, Q.G. Dai, Y.Q. Wang, Y. Guo, Y.L. Guo, Efficient low-temperature catalytic combustion of trichloroethylene over flower-like mesoporous Mn-doped CeO_2 microspheres, Appl. Catal. B-Environ. 102 (2011) 475–483.
[10] W. Wang, Q. Zhu, Q.G. Dai, X.Y. Wang, Fe doped CeO_2 nanosheets for catalytic oxidation of 1, 2-dichloroethane: effect of preparation method, Chem. Eng. J. 307 (2017) 1037–1046.
[11] Q.G. Dai, S.X. Bai, Z.Y. Wang, X.Y. Wang, G.Z. Lu, Catalytic combustion of chlorobenzene over Ru-doped ceria catalysts, Appl. Catal. B-Environ. 126 (2012) 64–75.
[12] Q.G. Dai, S.X. Bai, J.W. Wang, M. Li, X.Y. Wang, G.Z. Lu, The effect of TiO_2 doping on catalytic performances of Ru/CeO_2 catalysts during catalytic combustion of chlorobenzene, Appl. Catal. B-Environ. 142 (2013) 222–233.
[13] Q.G. Dai, L.L. Yin, S.X. Bai, W. Wang, X.Y. Wang, X.Q. Gong, G.Z. Lu, Catalytic total oxidation of 1, 2-dichloroethane over VO_x/CeO_2 catalysts: further insights via isotopic tracer techniques, Appl. Catal. B-Environ. 182 (2016) 598–610.
[14] Q.G. Dai, W. Wang, X.Y. Wang, G.Z. Lu, Sandwich-structured CeO_2@ZSM-5 hybrid composites for catalytic oxidation of 1, 2-dichloroethane: an integrated solution to coking and chlorine poisoning deactivation, Appl. Catal. B-Environ. 203 (2017) 31–42.
[15] Q.G. Dai, Z.Y. Zhang, J.R. Yan, J.Y. Wu, G. Johnson, W. Sun, X.Y. Wang, S. Zhang, W.C. Zhan, Phosphate-functionalized CeO_2 nanosheets for efficient catalytic oxidation of dichloromethane, Environ. Sci. Technol. 52 (2018) 13430–13437.
[16] X.P. Li, Y.L. Sun, Y.Y. Xu, Z.S. Chao, UV-resistant and thermally stable superhydrophobic CeO_2 nanotubes with high water adhesion, Small 14 (2018) 1801040–1801051.
[17] F. Bertinchamps, A. Attianese, M.M. Mestdagh, E.M. Gaigneaux, Catalysts for chlorinated VOCs abatement: multiple effects of water on the activity of VO_x based catalysts for the combustion of chlorobenzene, Catal. Today 112 (2006) 165–168.
[18] P.F. Sun, W.L. Wang, X.X. Dai, X.L. Weng, Z.B. Wu, Mechanism study on catalytic oxidation of chlorobenzene over $Mn_xCe_{1-x}O_2$/H-ZSM5 catalysts under dry and humid conditions, Appl. Catal. B-Environ. 198 (2016) 389–397.
[19] S.H. Peter, J.J. Yasser, S.E. William, D.J. Anker, V.W.J. Ton, Reversible and irreversible deactivation of Cu-CHA NH_3-SCRcatalysts by SO_2 and SO_3, Appl. Catal. B-Environ. 226 (2018) 38–45.
[20] A. Martínez-Hernández, G.A. Fuentes, S.A. Gómez, Selective catalytic reduction of NO_x with C_3H_8 using Co-ZSM5 and Co-MOR as catalysts: a model to account for the irreversible deactivation promoted by H_2O, Appl. Catal. B-Environ. 166-167 (2015) 465–474.
[21] Y.F. Feng, L. Wang, Y.H. Zhang, Y. Guo, Y.L. Guo, G.Z. Lu, Deactivation mechanism of $PdCl_2$-$CuCl_2/Al_2O_3$ catalysts for CO oxidation at low temperatures, Chin. J. Catal. 34 (2013) 923–931.
[22] Z. Hu, Z. Wang, Y. Guo, L. Wang, Y.L. Guo, J.S. Zhang, W.C. Zhan, Total oxidation of propane over a Ru/CeO_2 catalyst at low temperature, Environ. Sci. Technol. 52 (2018) 9531–9541.
[23] Q.G. Dai, S.X. Bai, H. Li, W. Liu, X.Y. Wang, G.Z. Lu, Catalytic total oxidation of 1, 2-dichloroethane over highly dispersed vanadia supported on CeO_2 nanobelts, Appl. Catal. B-Environ. 168–169 (2015) 141–155.
[24] V.K. Velisoju, G.B. Peddakasu, N. Gutta, V. Boosa, M. Kandula, K.V.R. Chary, V. Akula, Influence of support for Ru and water role on product selectivity in the vapor-phase hydrogenation of levulinic acid to γ-valerolactone: investigation by probe-adsorbed fourier transform infrared spectroscopy, J. Phys. Chem. C 122 (2018) 19670–19677.
[25] M.T. Chen, Y.F. Lin, L.F. Liao, C.F. Lien, J.L. Lin, Adsorption and reactions of CH_2Br_2 on TiO_2: effects of H_2O and O_2, Int. J. Photoenergy 6 (2004) 35–41.
[26] J. Saavedra, C.J. Pursell, B.D. Chandler, CO oxidation kinetics over Au/TiO_2 and Au/Al_2O_3 catalysts: evidence for a common water-assisted mechanism, J. Am. Chem. Soc. 140 (2018) 3712–3723.
[27] G.A. Olah, B. Gupta, M. Farina, J.D. Felberg, W.M. Ip, A. Husain, R. Karpeles, K. Lammertsma, A.K. Melhotra, N.J. Trivedi, Selective monohalogenation of methane over supported acidic or platinum metal catalysts and hydrolysis of methyl halides over γ-alumina-supported metal oxide/hydroxide catalysts. A feasible path for the oxidative conversion of methane into methyl alcohol/dimethyl ether, J. Am. Chem. Soc. 107 (1985) 7097–7105.
[28] J. He, T. Xu, Z. Wang, Q. Zhang, W. Deng, Y. Wang, Transformation of methane to propylene: a two-step reaction route catalyzed by modified CeO_2 nanocrystals and zeolites, Angew. Chem. Int. Ed. 51 (2012) 2438 –2442.
[29] C.W. Li, F. Hess, I. Djerdj, G.T. Chai, Y. Sun, Y.L. Guo, B.M. Smarsly, H. Over, The stabilizing effect of water and high reaction temperatures on the CeO_2-catalyst in the harsh HCl oxidation reaction, J. Catal. 357 (2018) 257–262.